A hyper-viscoelastic continuum model for preforming and consolidation of woven carbon fabric reinforced polymers (CFRPs)

Deyong Sun[1], Weizhao Zhang[1, 2#]

1 Department of Mechanical and Automation Engineering, The Chinese University of Hong Kong, Shatin, N.T., Hong Kong Special Administrative Region
2 Institute of Intelligent Design and Manufacturing, the Chinese University of Hong Kong
Corresponding Author / Email: weizhaozhang@cuhk.edu.hk (W. Zhang).

KEYWORDS: Preforming; Consolidation; Prepreg; Finite element method (FEM); Continuum model

The existing multiscale modeling methods for the performance of cured woven carbon fabric composites do not consider the thickness deformation and nonuniform resin distribution during processing of these materials, causing inaccuracy in numerical prediction. To enhance the modeling accuracy, this article presents a hyper-viscoelastic model using one-layer continuum elements to capture mechanics of the composite prepregs during both preforming and consolidation steps of the compression molding process. It can accurately predict the large deformation during preforming, including in-plane tension and shear, and out-plane bending. Moreover, the important thickness change due to in-plane shear before consolidation is also considered. In addition, the model can capture the significant thickness reduction and corresponding compression force during consolidation, which can potentially assist the mold design. To validate the hyper-viscoelastic model, preforming and consolidation simulation for benchmark single-dome and L-shape molds were conducted to analyze the predicted shear angle distribution, part geometry and part thickness after processing. In the future, this model will be utilized to explore the effects of resin flow, curing kinetics and temperature distribution on part performance and ultimately assist realization of the multiscale and integrated modeling for preforming, consolidation, curing and performance of woven CFRP parts manufactured via the prepreg compression molding.

NOMENCLATURE

w = internal potential energy
I_n = invariants based on deformation modes
$\mathbf{C}$ = the right Cauchy–Green strain tensor
$\boldsymbol{S}$ = second Piola-Kirchoff stress
$\boldsymbol{\sigma}$ = Cauchy stress tensor
$\boldsymbol{F}$ = deformation gradient
J = the determinate of the deformation gradient
i = the index number
F_{sh} = the normalized shear force
L = the initial length of specimen
d = the initial width of specimen

1. Introduction

Carbon fiber reinforced plastics (CFRPs) are one of the most promising materials for constructing lightweight vehicles because of their high performance-to-weight ratios and other superb performance [1, 2]. Among various advanced techniques for mass-production of CFRP parts, thermoforming has the highest application potential for its cost efficiency and freedom in part geometry [3]. CFRP thermoforming consists of preforming, compaction and curing and its whole manufacturing process can be found in Fig. 1. During preforming, woven prepreg sheets are heated for higher formability and deformed by a press in seconds [4]. In the following compaction step, the prepregs are compressed in closed metal molds with resin squeezed out from yarns and flow under elevated temperature and pressure within minutes [5]. Afterwards, the parts remained in compaction molds are cured under high temperatures and pressure usually for hours to solidify the resin [6]. Finally, post-processing can be applied to improve the geometrical accuracy of the parts [7]. Continuous manufacturing processes for thermoforming, including preforming, compaction, and curing, provide the initial states for the next steps.

The existing preforming simulation methods of woven reinforcements include kinematic, discrete and continuous models. The most popular method is continuous models, which consider the whole structure of prepregs as an equivalent homogenized continuous model and can be easily combined with commercial software. Several excellent continuous models have been proposed and verified by bias-extension and in-plane shear experiments, such as the hypo-elastic constitutive law [8], non-orthogonal constitutive models (uncoupled [9], and coupled [4] between in-plane tension and shear), and hyper-(visco)elastic model [10] for thermoset or thermoplastic prepregs. However, those models only focus on in-plane and bending behaviors during the forming processes and they are usually based on shell

elements considering the thin structure of prepregs. Hence, the through-the-thick behaviors and resin flow process are ignored with the assumption of thin plate theory.

In addition to thermoforming [11], the consolidation simulation models have been researched for automated fibre placement (AFP) [12], VARTM process (Vacuum Assisted Resin Transfer Molding) [13, 14], and autoclave [15, 16]. Xiong et al. [11] extended the hyper-viscoelastic model to the consolidation during thermoforming of thermoplastic composite prepregs based on solid-shell elements. It can efficiently simulate the thickness deformation of thin prepregs, but the effect of resin flow is omitted and only expressed by the viscosity during compaction. Belnoue et al. [17] combined a power flow model unlike the traditional flow model with hyper-viscoelastic constitutive law to classify the influence of shear flow and percolation flow on the macro performance of prepregs under consolidation, in which one-layer solid mesh was used to represent one-layer uncured prepreg. Mathieu et al. [18] developed the 3D hyperelastic model for interlock composite preforming. However, the real bending stiffness cannot be supported by weak transverse shear stiffness. Therefore, the second gradient hyperelastic orthotropic continuum model [19] was extended to provide internal bending force which can avoid spurious bending deformation. Sakhaei et al. [20] used the Cosserat continuum model to avoid spurious bending deformation by introducing additional rotational freedoms on the corner of solid elements, in which the hyperelastic model for the unidirectional dry fiber bed proposed by Gutowski et al. [21] was used to simulate the consolidation process. As mentioned in this article, this method can be inserted in the biphasic model as demonstrated in [15] to simulate the resin flow process. It is worth noting that a one-layer solid mesh was used to represent one-layer prepreg and cohesive elements were used on the surfaces of different layers. Weber et al. [22] made it possible for engineering application of a biphasic model in autoclave.

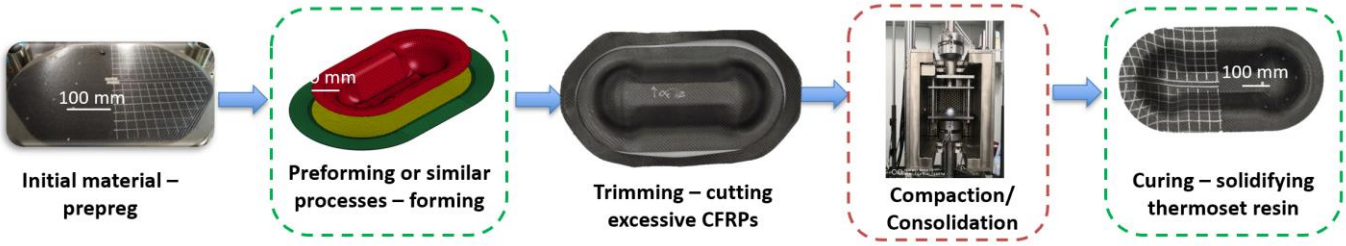

Fig. 1 Thermoforming manufacturing process.

The consolidation phase is significant to the performance of the final parts. During this step, high pressure is applied on the heated prepregs to ensure good cohesion between fibers and resin by removing the inter- and intra-layer porosities. Meanwhile, the initial states introduced by preforming will significantly influence the consolidation property of prepregs, especially nonuniform yarn angle, thickness, and stress. As shown in Fig. 2 (a), when the selected commercial-grade prepregs are sheared to a 30° yarn angle, their thickness can increase by nearly 60% due to variations of fabric architecture. The non-uniform prepreg thickness, together with the change of fabric permeability, can then significantly affect pressure during compaction and curing to achieve the target part thickness. Experimental results in Fig 2. (b) illustrate that 0.3 bar of pressure can reduce the thickness of the original orthogonal prepregs by around 11.3% after compaction and curing. However, the prepregs with a 60° yarn angle require 0.6 bar for similar thickness. For prepregs with a 30° yarn angle, even 5 bar is far from adequate for the target compression. CFRP thermoforming utilizes closed molds made of stiff metal to preform and compress prepregs to realize complex part geometry and smooth surface finish. Therefore, if the design of both mold and process does not thoroughly consider the relationship among nonuniform pressure field, mold gap and part thickness throughout the complex 3D space for thermoforming,

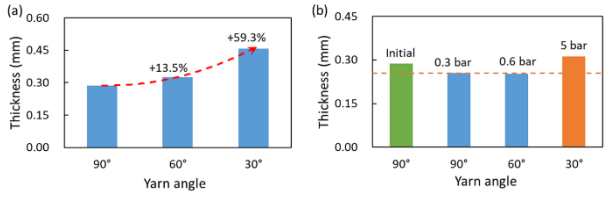

Fig. 2 Thickness of the selected commercial-grade woven prepregs after being (a) sheared to various yarn angles, and then (b) compacted and cured under different pressure.

insufficient pressure will be applied to certain regions on parts during compaction and curing, leading to incomplete resin squeeze-out from yarns and partial immersion of fabric architecture, which in turn will cause rough fabric surfaces and even yarn separation as demonstrated in Fig. 3 (a) and (b), respectively, especially when combined with the chemical shrinkage induced by curing. These manufacturing defects will greatly impair surface finish, and even more seriously, the performance of parts as load cannot be effectively transferred among yarns via resin matrix. The purpose of this article is to propose a numerical model to simulate the prepreg consolidation process in thermoforming to optimize the time consumption and pressure and to obtain excellent performance CFRP parts with smooth surface as shown in Fig. 3 (c). More importantly, this consolidation model can inherit the non-uniform and non-orthogonal properties of prepregs from preforming step and will be used to study the yarn separation and residual stress caused by the chemical shrinkage of resin under curing.

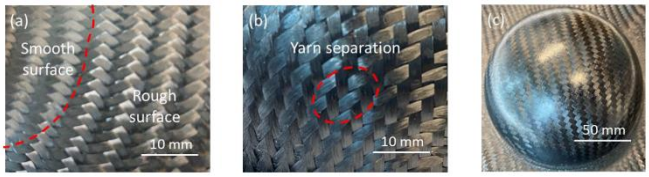

Fig. 3 Insufficient thermoforming pressure and chemical shrinkage during curing causes (a) rough fabric surface, and (b) yarn separation in a single-dome part. The high-quality part in (c) demonstrates smooth surface, and well-integrated carbon fiber yarns and resin matrix.

Based on the aforementioned issues, the biphasic model must be used in order to simultaneously simulate the thickness deformation and resin flow process under consolidation of thermoforming, in which the non-orthogonal constitutive model of fiber bed as the skeleton and non-uniform permeability should be inherited from preforming. Meanwhile, it is worth noticing that the biphasic model is based on solid (continuum) elements. Hence, section 2 developed the hyperelastic model for preforming of the uncured thin prepregs based on one-layer solid mesh. Section 3 described the numerical verification of the current method by single dome thermoforming. Conclusions and future

work will be discussed in section 4.

2. Framework of preforming and consolidation model for uncured prepreg

2.1 Anisotropic hyperelastic model under large deformation

The hyperelastic law is built based on the 3D interlock model [18]. For the integrity of this article, some basic methods are written here. More details can be found in Ref. [18]. For hyperelastic materials with an anisotropic response, the anisotropy is simply embodied in the potential w, providing a natural framework for a frame-invariant formulation:

$$w(\mathbf{C}) = w(I_1, I_2, ..., I_n) \tag{2.1}$$

The considered deformation modes can be found in Fig. 4 and they are controlled by decoupled invariants. Hence, the volume strain energy can be expressed as the sum of different energies depending on the related frame invariants.

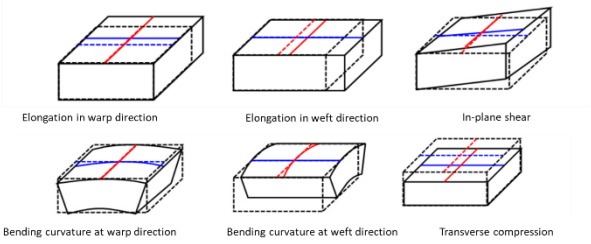

Fig. 4 Deformation modes for woven reinforcement within a hyperelastic framework. [18]

$$\begin{aligned} w = {} & w_{elong1}(I_{elong1}) + w_{elong2}(I_{elong2}) \\ & + w_{\text{in}-plane\ shear}(I_{shear12}) + w_{out-plane\ shear}(I_{shear13}, I_{shear23}) \\ & + w_{bend}(I_{\chi}) + w_{comp}(I_{comp}) \end{aligned} \tag{2.2}$$

All of the details about the definition of various invariants can also be found in Ref. [18]. Unlike the 3D interlock composites, the deformation of the thin prepreg during preforming only considering in-plane elongation, in-plane shear, out-plane compaction, and bending. The transverse deformation introduced by out-plane shear deformation is not important for thin prepreg, which provides another freedom to avoid spurious bending deformation because of the small out-plane shear stiffness [23]. That means the out-plane shear stiffness can be enhanced manually to fix the spurious bending deformation.

The second Piola-Kirchoff stress $\boldsymbol{S}$ can be derived from the internal energy w by the right Cauchy-Green strain tensor $\boldsymbol{C}$.

$$\mathbf{S} = 2\frac{\partial w(\mathbf{C})}{\partial \mathbf{C}} \tag{2.3}$$

The Cauchy stress tensor $\boldsymbol{\sigma}$ can be obtained with the deformation gradient $\boldsymbol{F}$.

$$\boldsymbol{\sigma} = \frac{1}{J}\mathbf{F}\mathbf{S}\mathbf{F}^T \tag{2.4}$$

To explicitly express the Cauchy stress as in Eq. (2.4), the decoupled energy functions are usually expressed as polynomial functions, each of which is expressed as follows:

$$w(I) = \sum_{i=1}^{6} k_i \mid I \mid^{i+1} \tag{2.5}$$

2.2 Material properties identification

Many details about the experiments for preforming can be found in our previous work [24] and the related data processing method can be found in Ref. [25]. Here only shows the difference between our one-layer continuum model and the traditional method.

2.2.1 Uniaxial tensile

The average experiment data about uniaxial tension for heated prepregs under 70°C can be found in Fig. 5. To accurately describe

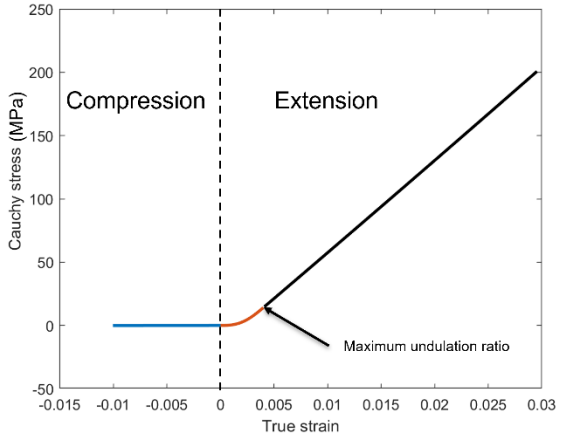

Fig. 5 Stress-strain curve for uniaxial extension.

the smooth stress-strain relationship, the C^2 continuity energy function for uniaxial extension is set as following:

$$w = \begin{cases} k_1 I^2 + k_2 I^3 + k_3 I^4 + k_4 I^5 + k_5 I^6 + k_6 I^7, & I < 0 \\ k_1 I^2 + k_7 I^3 + k_8 I^4 + k_9 I^5 + k_{10} I^6 + k_{11} I^7, & 0 \le I \le I_0 \\ w(I_0) + \left.\frac{\partial w}{\partial I}\right|_{I=I_0} (I - I_0) + \frac{1}{2}\left.\frac{\partial^2 w}{\partial I \partial I}\right|_{I=I_0} (I - I_0)^2, & I > I_0 \end{cases} \tag{2.6}$$

where I_0 is the maximum undulation ratio.

2.2.2 Bias-extension

The shearing related parameters in the hyperelastic model can be verified from the bias-extension test. It would be easily

facilitated compared with the picture frame test. The experiments have demonstrated the shearing properties of thermoset prepregs are hyperelastic rather than hyper-viscoelastic. Noticed that the bias-extension test contains the coupled effect between in-plane tension and in-plane shear, but the internal energy functions are decoupled. Hence, the in-plane shear force must be separated before the confirmation of in-plane shear properties.

Cao et al. [26] proposed a function to evaluate the normalized shear force F_{sh} as following:

$$F_{sh}(\gamma)=\frac{1}{(2L-3d)\cos\gamma}\left[(\frac{L}{d}-1)F(\cos\frac{\gamma}{2}-\sin\frac{\gamma}{2})-dF_{sh}(\frac{\gamma}{2})\cos\frac{\gamma}{2}\right] \quad (2.7)$$

in which, L and d are the initial length and width of the specimen, γ is the shear angle, and F is the clamping force under the bias-extension test. Hence, the pure in-plane shear parameters can be verified as shown in Eq. (2.4).

2.2.3 Out-plane compaction behavior

As discussed before, the in-plane shear will influence the thickness and compaction stiffness mainly because of the yarn angle variation. During the consolidation stage, the fiber bed's elastic behavior and viscous resin flow, especially the resin percolation and squeezing flow, will cause the viscoelastic effect on molten prepregs. This phenomenon often called as flow-dependent viscoelasticity. Meanwhile, the squeeze out of resin from prepregs, combined by the incompressible fiber bed and resin, will make the prepreg compressible. Therefore, two general methods are often explored by global researchers, one is hyper-viscoelastic model without considering resin flow, the other one is called biphasic model. Anyway, the hyper-viscoelastic constitutive law can be built firstly to explore the thickness deformation. The time dependent stress can be expressed by Prony series as a convolution integral [27].

2.2.4 Out-plane bending behavior

Unlike the traditional preforming method based on shell mesh, in which bending behavior is controlled by specified transverse shear stiffness. The out-plane shear parameters should be calibrated by Bayesian model [28] after confirming the previous parameters. Those out-plane shear properties don't need to be tested by experiments and cannot influence other deformation modes.

3. Numerical model validation

3.1 Bias-extension simulation

To validate the proposed hyper-viscoelastic model, the bias-extension deformation was simulated by C3D8R in ABAQUS/Explicit with the default hourglass control. Fig. 6 (a) shows that the excellent coincidence between experiment and simulation at correct out-plane shear stiffness. However, the local wrinkles will appear at low out-plane shear stiffness as shown in

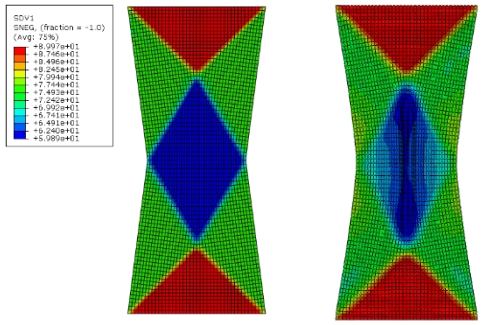

(a) (b)

Fig. 6 Yarn angle in bias-extension simulation. (a) without wrinkle (b) with wrinkle.

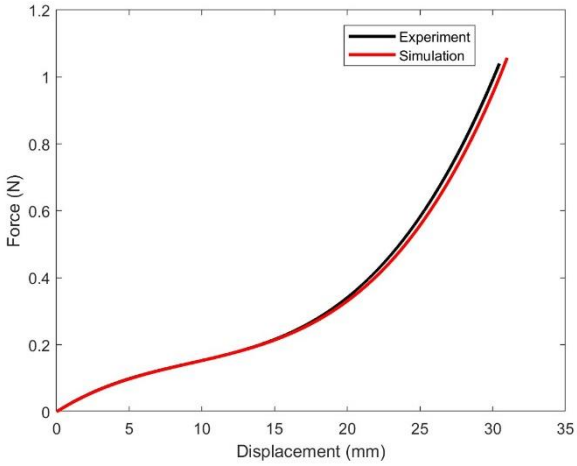

Fig. 7 Comparison of load-displacement curve.

Fig. 6 (b). Comparison of force-displacement curve in bias-extension test is shown in Fig. 7. The load-displacement curve obtained from the simulation is fairly close but little lower than the experiment result.

3.2 Out-plane bending simulation

The out-plane bending simulation will be done after completing the calibration of out-plane shear properties as discussed in section 2.2.4.

3.3 Single dome thermoforming simulation

Single dome [25] and double dome [11] as the forming benchmarks have been investigated at many aspects of the dry fabrics and pre-impregnated reinforcements. Fig. 8 shows the half of the FE model for symmetric reasons. The punch with radius of 49.2 mm will move with an average speed of 6m/s. The die with radius of 50 mm is fixed on its initial location. The binder will provide the blank holder force of 200N at the whole process. The rectangular specimen with size of 200mm×200mm×0.32mm is discretized by C3D8R element and only one-layer solid element is located on the thickness direction. Other rigid parts are discretized by R3D4 element. The blank was orientated at 0/90° in global coordinates. The whole thermoforming process was simulated by

Abaqus/Explicit. Meanwhile, the friction coefficient was set as 0.212 according to experiment tests at 70°C. Isothermal and homogeneous distribution assumptions were made during the simulations, and the temperature was fixed at 70°C based on manufacturing processes. The objective of this simulation was to investigate the ability of one-layer solid mesh on simulating the evolution of consolidation during thermoforming steps.

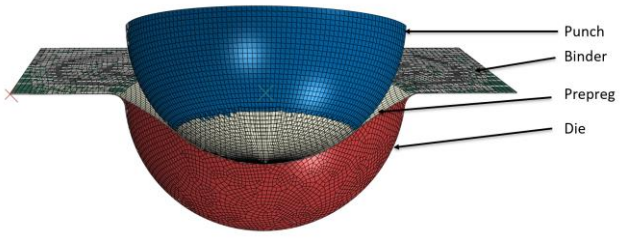

Fig. 8 Simulated FE model (1/2 model)

Figs. 9-11 show the Mises stress distribution, yarn angle and thickness before and after compaction respectively. The status before compaction is defined at the moment when the specimen contacted with die. The status after compaction is defined as the punch moved down 0.1mm again. The enhanced Mises stresses as shown in Fig. 9(b) reflected the high compaction force compared with the preforming process. The small yarn angle difference between Fig. 10(a) and Fig. 10(b) reflects the little deformation during compaction stage. The large thickness deformation and its non-uniform distribution during consolidation can be found in Fig. 11(b), which has significant difference with Fig. 11(a).

4. Conclusions

Consolidation is one of the crucial steps of thermoforming, which determines the thickness and volume fraction of fibers in the cured CFRP parts. All of them will significantly influence the performance of CFRPs. The existing multiscale modeling methods [29] for the performance of cured woven carbon fabric composites do not consider the thickness deformation and nonuniform resin distribution during processing of these materials, causing inaccuracy in numerical prediction. In this article, the hyper-viscoelastic model using one-layer continuum elements to capture mechanics of the composite prepregs during both preforming and consolidation steps of the compression molding process. Meanwhile, the computational efficiency will keep because of the use of 3D reduced integral elements compared to traditional shell element.

More importantly, the status after preforming can be transformed into consolidation and curing directly, especially the anisotropic constitutive law, thickness and stress. Meanwhile, the current model can also be used in biphasic model to explore the resin redistribution under compaction, which cannot be done by previous consolidation model [11] of thermoforming. Therefore, the residual stress and fiber separation from chemical shrinkage of resin during curing can also be simulated. Then a more realistic multiscale modeling method can be built by considering the residual stress, non-uniform thickness and volume fraction of fibers simultaneously. Finally, this numerical model can assist the thermoforming manufacturing process design, such as compaction force, time consumption and temperature by predicting their influence on the final performance of CFRPs accurately.

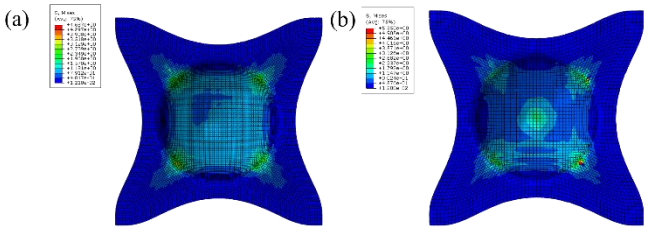

Fig. 9 The Mises stress distribution (a) before compaction (b) after compaction.

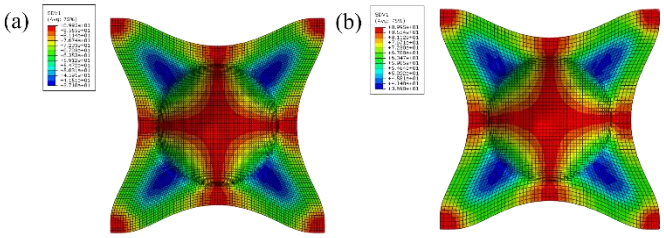

Fig. 10 The yarn angle distribution (a) before compaction (b) after compaction.

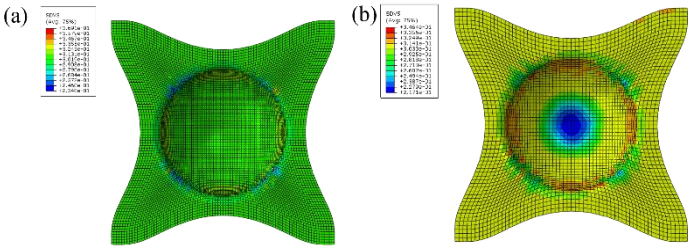

Fig. 11 The thickness distribution (a) before compaction (b) after compaction.

ACKNOWLEDGEMENT

The work described in this paper was supported by grants from CUHK Vice-Chancellor's PhD Scholarship.

REFERENCES

1. Che, D., et al., *Machining of Carbon Fiber Reinforced Plastics/Polymers: A Literature Review.* Journal of Manufacturing Science and Engineering, 2014. **136**(3).
2. Wang, M., Q. Kang, and N. Pan, *Thermal conductivity enhancement of carbon fiber composites.* Applied Thermal Engineering, 2009. **29**(2-3): p. 418-421.
3. Hsiao, S.-W. and N. Kikuchi, *Numerical analysis and optimal design of composite thermoforming process.* Computer methods in applied mechanics and engineering, 1999. **177**(1-2): p. 1-34.
4. Zhang, W., et al., *A non-orthogonal material model of woven composites in the preforming process.* CIRP Annals, 2017. **66**(1): p. 257-260.

5. Bublitz, D., D. Colin, and K. Drechsler, *Implementation of a viscoelastic material model to predict the compaction response of dry carbon fiber preforms.* Composites Part A: Applied Science and Manufacturing, 2022. **153**.
6. Feng, Y., et al., *Numerical modeling for curing of unidirectional carbon fiber reinforced polymer based on micromechanics in Laplace domain.* Composites Science and Technology, 2022. **228**: p. 109637.
7. Zhang, W., J. Gao, and J. Cao, *Blank geometry design for carbon fiber reinforced plastic (CFRP) preforming using finite element analysis (FEA).* Procedia Manufacturing, 2020. **48**: p. 197-203.
8. Khan, M.A., et al., *Numerical and experimental analyses of woven composite reinforcement forming using a hypoelastic behaviour. Application to the double dome benchmark.* Journal of Materials Processing Technology, 2010. **210**(2): p. 378-388.
9. Xue, P., X. Peng, and J. Cao, *A non-orthogonal constitutive model for characterizing woven composites.* Composites Part A: Applied Science and Manufacturing, 2003. **34**(2): p. 183-193.
10. Charmetant, A., et al., *Hyperelastic model for large deformation analyses of 3D interlock composite preforms.* Composites Science and Technology, 2012. **72**(12): p. 1352-1360.
11. Xiong, H., N. Hamila, and P. Boisse, *Consolidation Modeling during Thermoforming of Thermoplastic Composite Prepregs.* Materials (Basel), 2019. **12**(18).
12. Valverde, M.A., et al., *Compaction behaviour of continuous fibre-reinforced thermoplastic composites under rapid processing conditions.* Composites Part A: Applied Science and Manufacturing, 2021. **149**.
13. Pillai, K.M., C.L. Tucker, and F.R. Phelan, *Numerical simulation of injection/compression liquid composite molding. Part 2: preform compression.* Composites Part A: Applied Science and Manufacturing, 2001. **32**(2): p. 207-220.
14. Pillai, K.M., C.L. Tucker, and F.R. Phelan, *Numerical simulation of injection/compression liquid composite molding. Part 1. Mesh generation.* Composites Part A: Applied Science and Manufacturing, 2000. **31**(1): p. 87-94.
15. Li, M. and C.L. Tucker, *Modeling and simulation of two-dimensional consolidation for thermoset matrix composites.* Composites Part A: Applied Science and Manufacturing, 2002. **33**(6): p. 877-892.
16. Chan, C., *Compaction Simulation for Prepreg-AutoclaveManufacturing: Improvements and Simplifications of Two Compaction Simulation Methodologies*. 2019.
17. Belnoue, J.P.H., et al., *A novel hyper-viscoelastic model for consolidation of toughened prepregs under processing conditions.* Mechanics of Materials, 2016. **97**: p. 118-134.
18. Mathieu, S., et al., *Enhanced modeling of 3D composite preform deformations taking into account local fiber bending stiffness.* Composites Science and Technology, 2015. **117**: p. 322-333.
19. Madeo, A., et al., *Thick fibrous composite reinforcements behave as special second-gradient materials: three-point bending of 3D interlocks.* Zeitschrift für angewandte Mathematik und Physik, 2015. **66**(4): p. 2041-2060.
20. Sakhaei, A.H., S. Erland, and T.J. Dodwell, *A finite deformation Cosserat continuum model for uncured carbon fibre composites.* Mechanics of Materials, 2020. **151**.
21. Gutowski, T.G., et al., *Consolidation Experiments for Laminate Composites.* Journal of Composite Materials, 1987. **21**(7): p. 650-669.
22. Weber, T.A., *Herstellprozesssimulation zur Vorhersage der Faltenbildung in der Prepreg-Autoklav-Fertigung*. 2018, Dissertation, Kaiserslautern, Technische Universität Kaiserslautern, 2017.
23. Boisse, P., N. Hamila, and A. Madeo, *The difficulties in modeling the mechanical behavior of textile composite reinforcements with standard continuum mechanics of Cauchy. Some possible remedies.* International Journal of Solids and Structures, 2018. **154**: p. 55-65.
24. Zhang, W., et al., *Experimental methods to characterize the woven composite prepreg behavior during the preforming process*. 2016, Ford Motor Company, Detroit, MI (United States).
25. Gao, S.S., et al., *An efficient hyper-elastic model for the preforming simulation of Carbon-Kevlar hybrid woven reinforcement.* Chinese Journal of Aeronautics, 2022. **35**(12): p. 321-335.
26. Cao, J., et al., *Characterization of mechanical behavior of woven fabrics: Experimental methods and benchmark results.* Composites Part A: Applied Science and Manufacturing, 2008. **39**(6): p. 1037-1053.
27. Ghorbanoghli, A. and K. Narooei, *A new hyper-viscoelastic model for investigating rate dependent mechanical behavior of dual cross link self-healing hydrogel.* International Journal of Mechanical Sciences, 2019. **159**: p. 278-286.
28. Zhang, W., et al., *A numerical Bayesian-calibrated characterization method for multiscale prepreg preforming simulations with tension-shear coupling.* Composites Science and Technology, 2019. **170**: p. 15-24.
29. Liang, B., et al., *Multi-scale modeling of mechanical behavior of cured woven textile composites accounting for the influence of yarn angle variation.* Composites Part a-Applied Science and Manufacturing, 2019. **124**.